P. et al. Protection and Control of Modern Power Systems (2018) 3:14
https://doi.org/10.1186/s41601-018-0082-4

Protection and Control of Modern Power Systems

ORIGINAL RESEARCH Open Access

Robust fault analysis in transmission lines using Synchrophasor measurements

Rajaraman P.[1], Sundaravaradan N.A.[2], Mallikarjuna B.[3], Jaya Bharata Reddy M.[3*] and Mohanta D.K.[4]

Abstract

As more electric utilities and transmission system operators move toward the smart grid concept, robust fault analysis has become increasingly complex. This paper proposes a methodology for the detection, classification, and localization of transmission line faults using Synchrophasor measurements. The technique involves the extraction of phasors from the instantaneous three-phase voltages and currents at each bus in the system which are then decomposed into their symmetrical components. These components are sent to the phasor data concentrator (PDC) for real-time fault analysis, which is completed within 2–3 cycles after fault inception. The advantages of this technique are its accuracy and speed, so that fault information may be appropriately communicated to facilitate system restoration. The proposed algorithm is independent of the transmission system topology and displays high accuracy in its results, even with varying parameters such as fault distance, fault inception angle and fault impedance. The proposed algorithm is validated using a three-bus system as well as the Western System Coordinating Council (WSCC) nine bus system. The proposed algorithm is shown to accurately detect the faulted line and classify the fault in all the test cases presented.

Keywords: Transmission line faults, Fault analysis, Phasor measurement units, Symmetrical components

1 Introduction

The widespread integration of new high-voltage transmission in the scenario of modern power systems has necessitated the need for an efficient wide-area protection system (WAPS). Since transmission lines span large areas, the chances of a fault occurring in transmission lines are also very high, which compromises system reliability [1]. WAPS are incorporated in modern power grid networks to monitor and detect any anomalies across large areas of the power system to ensure the reliable operation of the system. Transmission line fault analysis is, therefore, a crucial part of the operation of power systems. In this regard, this paper proposes a robust technique for the detection, classification, and location of transmission line faults based on the analysis of symmetrical components of voltage and current phasors.

Much of the previous works [2–5] in fault analysis in power systems possess the inherent disadvantage of the strong dependence on the network configuration. The usage of wavelet transform extends to its collaboration with soft computing techniques for fault analysis, as reported in [6, 7]. However, these techniques are highly dependent on the system parameters and cannot be applied when the system topology changes. Utilisation of soft computing techniques such as neural networks and fuzzy logic [8, 9] has also been of significant research interest in power system fault analysis due to their learning capability to recognize fault events. Neural networks were adopted in many fields of power system operation to improve real-time protection of transmission lines [10–13], but they depend on system parameters, and it is cumbersome to efficiently train a neural network to recognize fault occurrences in large/ interconnected power systems.

The introduction of phasor measurement units (PMUs) revolutionized the research in power system measurement and control [14–28]. The wide range of techniques for the incorporation of PMUs in power system protection has been reported by Ramesh et al. [14]. Phadke et al. [15] have proposed a fault detection scheme based on sequence components of voltage and current phasors, but the work is limited to a two-bus

* Correspondence: jayabharat_res@yahoo.co.in
[3]Department of Electrical and Electronics Engineering, National Institute of Technology, Tiruchirappalli, Tamilnadu 620015, India
Full list of author information is available at the end of the article

system and does not encompass fault classification and localization algorithms.

In recent works, there has been a strong focus on optimal PMU placement for power system observability and protection [22, 23], but most of these methodologies need an instantaneous static state estimation of the power system either through circuit breaker status or zonal protection status or both. In [24], the authors have proposed a fault location methodology under dynamic conditions wherein the spatial and temporal features of the line voltages and currents are preserved to get dynamic phasor estimates to perform fault location. However, such techniques may not be fast, and the accuracy and resilience of the proposed algorithm in physical line models have not been validated. Other recent works [25–28] have focused on the optimal placement of PMUs in electric grids to minimize investment costs and reduce uncertainty in measurements. In [23], the authors have performed adaptive fault analysis by dividing the system into backup protection zones, and then using the value of the zero and positive sequence current components to detect the presence of a fault. However, the study does not indicate the ability to distinguish line faults from other transient events. In [25], the authors have performed accurate fault analysis using data obtained from a PMU device located at only one bus in the transmission system. Such an approach is economical and reduces the impacts of measurement errors. The voltage and current phasors at all buses in the system are computed using the data from a single PMU device, and the fault analysis procedure is implemented. Optimal PMU placement techniques depend on the severity of contingencies that are considered, and sufficient measurements must be available for the accurate detection and classification of transmission faults. However, these works do not account for complete system observability for all possible contingencies, and the impacts of PMU device outages may be severe in certain contingencies.

Some papers on optimal PMU placement for power system protection have adopted probabilistic approaches [26, 27] to account for highly probable system contingencies. These works focus on the placement of PMUs at the most reliable buses to minimize the number of required measurements to perform fault analysis. For instance, the authors in [27] formulate a reliability-based PMU placement problem based on the most credible contingencies, but this approach may not work in all power system contingencies, and the measurements may not be sufficient to distinguish transmission line faults from other transient events accurately. The fault analysis procedure is also computationally intensive and may be in the order of 8–10 cycles of the nominal frequency.

Hence, an efficient fault analysis algorithm using phasor quantities and high-speed processors is developed and validated through experimental results. The proposed algorithm is equipped to distinguish between permanent line faults and other transient events in the transmission line. Our study also considers several fault parameters such as the fault impedance, fault inception angle (FIA) and location of the fault, and our algorithm is shown to be immune to variations in these parameters. The entire fault analysis procedure is completed within 3–5 cycles of the nominal frequency, which exhibits the robustness and speed of our algorithm. The major contribution of our work is its universal applicability to any power network topology, which is an important advantage as many conventional techniques are designed for specific network topologies or specific types of power system contingencies.

2 Phasor measurement units

A phasor is a vector quantity which is used to represent a sinusoidal signal regarding its magnitude and phase angle. The magnitude of the phasor is equal to the Root Mean Square (RMS) value of the sinusoidal signal.

PMUs are placed at each bus in a power system and are used to measure the instantaneous voltages and currents in a large network using a Global Positioning System (GPS) synchronized time source for data synchronization. This time synchronization source provides for the synchronization of real-time measurements at remote points in the network. The analog data obtained in the individual PMUs in a power network are converted to their equivalent phasors and sent via high-speed communication channels to the PDC. At the PDC, phasor data received from different PMUs connected to all buses in the power network are used to initiate wide-area protection, control, and monitoring actions. This synchronized phasor data provides the distinct advantage of incorporating fault analysis techniques in any power system. In this paper, it is assumed that an excellent communication channel is available via optical fiber cables for transfer of data from the PMUs to the PDC.

The Discrete Fourier Transform (DFT) is used to compute the phasor quantities from the original analog signals. The input analog signal (x(t), which denotes the three-phase voltage/current signal) is sampled at a specified sampling frequency (N samples/cycle). Within a cycle, a phasor is estimated by applying the DFT on N samples over a running window of one cycle of the fundamental frequency (as shown in eq. 1). Successive phasors are estimated by applying DFT on a new set of samples which are obtained by discarding the first value in the previous sample window and taking the next sample in the successive sample window. The RMS value of the DFT output is taken as the magnitude of the phasor

quantity. For discerning transient events, the DFT outputs are continuously generated to provide the phasor outputs. The phasors that are obtained will be sent via communication channels to the PDC for fault analysis.

$$X(k) = \sum_{n=0}^{N-1} x(n) e^{\frac{-j2\pi nk}{N}}, k \in [0, N-1] \quad (1)$$

In a polyphase system, asymmetrical faults are more complicated to analyze as the voltage, and current magnitudes in all the phases will not be equal. In the proposed algorithm, the three-phase phasor quantities are decomposed into their symmetrical components for analysis. Fig. 1 depicts the methodology incorporated in the proposed work.

3 Fault detection strategy using PMUs

Each substation in the power system has potential transformers (PT) and current transformers (CT) to monitor the three-phase bus voltages and line currents. PTs are placed at each bus to measure the bus voltage and CTs are placed at both ends of each line connected to all the buses. The PT and CT are connected to a PMU at the corresponding bus. The PMUs convert these analog quantities to their equivalent phasor quantities and transmit them to the Phasor Data Concentrator (PDC).

If a disturbance occurs and happens to be an asymmetric fault, there will be negative sequence components introduced in the bus voltages and line currents. However, there is a complete absence of these sequential components in case of a symmetric fault. In case of a symmetric fault, the positive sequence current phasor magnitude will be much higher than its normal operating value. Therefore, keeping in mind the possibility of occurrence of both these types of faults, the fulfillment of at least one of these conditions must be checked. The proposed algorithm to determine the faulted bus is shown in Fig. 2.

The first step in the proposed algorithm is to check whether there is a presence of negative sequence voltage

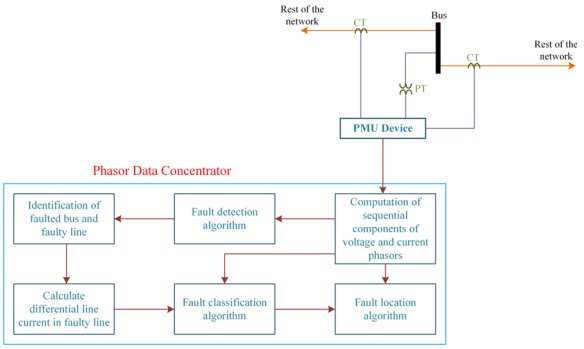

Fig. 1 Block diagram of Proposed Fault Analysis Procedure

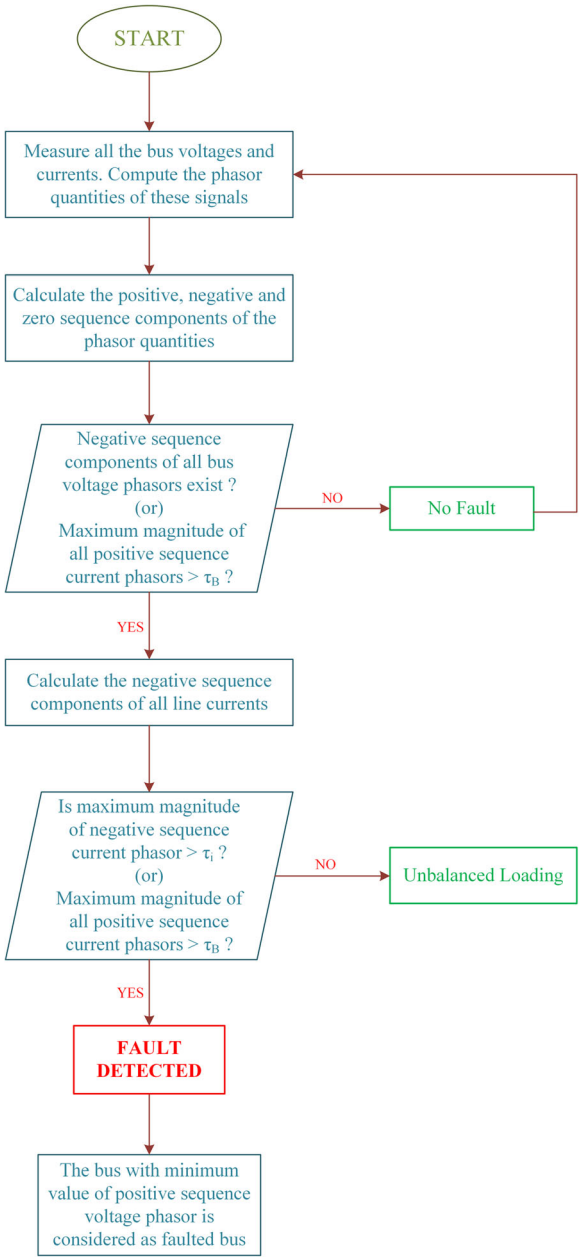

Fig. 2 Fault Detection Algorithm

phasor components at all the buses in the system, or if the maximum value of the positive sequence current phasors exceeds a threshold limit (τ_B). If one of these two conditions is satisfied, it confirms the presence of either a line fault or unbalanced loading. As long as neither of these conditions is satisfied, there is no fault in the system. The value of τ_B is taken to be 1.5 p.u (based on experimental results) for the three-bus system that is considered for demonstrating the algorithm. In practice, most of the EHV transmission lines are modeled and analyzed before they are installed and commissioned. Hence, the line parameters are easily available.

By using this data, simulation studies can be performed to determine the threshold values for the fault detection and classification algorithms. The threshold value is set such that the algorithm ignores power system transients.

The discrimination between a fault and unbalanced loading can be performed by computing the negative sequence components of all the current phasors in all lines of the system. If the maximum magnitude of the negative sequence current phasor is greater than a threshold (τ_i), this indicates the presence of a fault. The value of τ_i is experimentally computed to be 0.3 p.u for the three-bus system considered for demonstrating the algorithm. If this condition is not satisfied, it indicates unbalanced loading in the system. (If there is a presence of unbalanced loading, it is indicated by the algorithm but is not considered as a fault). In case of a fault indication, the bus with the least value of positive sequence voltage phasor magnitude is termed as the faulted bus. In this paper, the faulted bus is one of the buses which is connected to the faulty branch. It is the bus which has the least value of positive sequence voltage phasor magnitude among all buses in the system. When a fault occurs in a transmission line system, the voltages at the buses connected to the faulted line drop, which leads to large currents flowing through the other phases, and even neighboring lines. Hence, this large voltage drop requires the circuit breakers to act quickly to remove the faulted line to restore the stability of the system. For no other transient events does the voltage of the bus drop very low permanently; else the entire system would become unstable. Once the faulted bus is identified according to our algorithm, the faulty branch is then identified.

We denote the identified faulty bus as bus *i*. Let S be the set of all branches connected to bus *i*. For the faulty branch detection algorithm (presented in Fig. 3), only the lines *i-j* which are connected to the faulted bus *i* are considered to reduce the computational time. For locating the faulty branch *i-j*, the differences of positive sequence current phasor angles measured at both ends of the lines (connected to the faulted bus) are computed and is denoted by θ_{cpij}. The maximum value of θ_{cpij} among all the positive sequence current phasor angles is considered as the faulty branch. In a faulty branch, the difference between the positive sequence current phasor angles at both ends of the faulty branch would be larger than the corresponding values in the healthy branches.

For validating the proposed fault detection algorithm, a case study with a three-bus system is considered. The following system parameters are considered for this study: one generator bus (hereafter denoted as bus 1) having a rating of 400 kV, 50 Hz and the load buses (bus 2 and bus 3) having a total power rating of 300 MVA. These three buses are interconnected with 3 Extra High Voltage (EHV) transmission lines, which are modeled in MATLAB - SIMULINK.

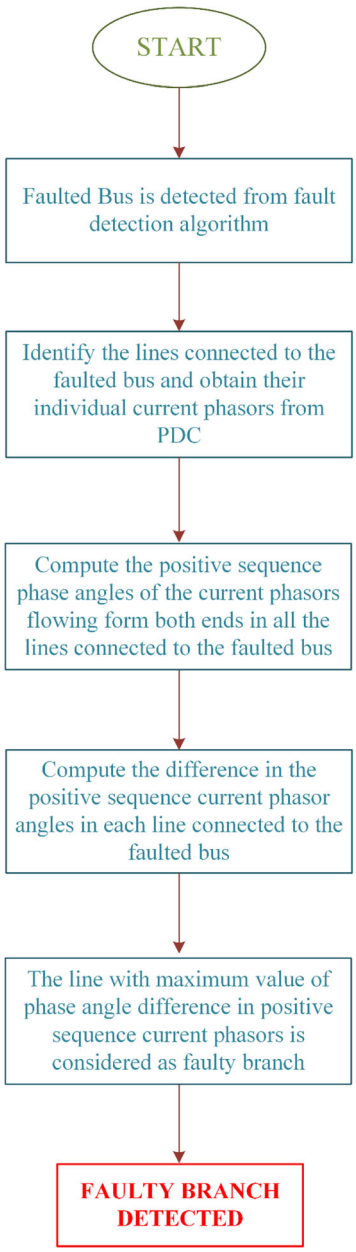

Fig. 3 Faulty Branch Detection Algorithm

The positive and negative sequence parameters of the line resistance, line inductance, and line capacitance are $R = 0.01273\ \Omega$/km, L = 0.9337 mH/km and C = 12.74 nF/km respectively. The zero sequence parameters of the line resistance, line inductance, and line capacitance are $R_0 = 0.3864\ \Omega$/km, $L_0 = 4.1264$ mH/km and $C_0 = 7.751$ nF/km respectively [24]. The line lengths are taken as 200 km for each line. For the given 300 MVA, 400 kV system, the threshold values τ_i and τ_B can be calculated as 0.13kA (0.3 p.u) and 0.65 kA (1.5 p.u) respectively.

Fig. 4(a) shows the voltage waveform for ABG fault in line 2–3 in the power system.

The fault detection algorithm operates within 8–10 ms (less than half a cycle), as shown in Fig. 4(b). The single line diagram of the prescribed three-bus system is shown in Fig. 5. Unbalances in the system should not be mistaken as faults and the algorithm is resilient to such transient events.

A study involving LG fault is presented in Table 1 for validating the fault detection algorithm. A case of a BG fault at 90 km (from Bus 2) in line 2–3 is considered (Table 1). The fault impedance considered is 10 Ω. As the magnitudes of individual negative sequence components of bus voltage phasors (V_1^-, V_2^- and V_3^-) are greater than zero, it indicates the presence of unbalanced loading or a fault. Next, it is observed that the maximum magnitude of the negative sequence component (I_{Max}^-) is 1.33 kA, which is greater than the threshold value (τ_i) which is 0.225 kA. This condition indicates the presence of a fault (not an unbalanced loading condition) and the next step is to identify the faulted bus. For obtaining this, the values of the positive sequence voltage phasor magnitudes at buses 1, 2 and 3 are obtained as $V_1^+ = 375.63$ kV, $V_2^+ = 371.25$ kV and $V_3^+ = 370.06$ kV respectively. The faulted bus in the system is Bus 3, as it has the least value of positive sequence voltage phasor magnitude.

For locating the faulty branch, the difference in positive sequence current phasor angles measured at both ends of the lines (connected to the faulted bus) are computed. Since the faulted bus is detected as Bus 3, only line 2–3 and line 3–1 are considered. For making the process

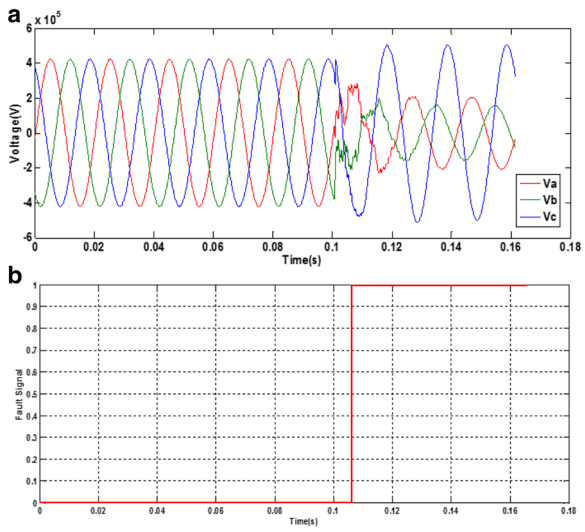

Fig. 4 (**a**) Voltage at Bus 3 for an ABG fault created in line 2–3 in the three-bus model at 0.1 s, (**b**) Fault Detection Signal for the ABG fault created in line 2–3 in the three-bus model at 0.1 s

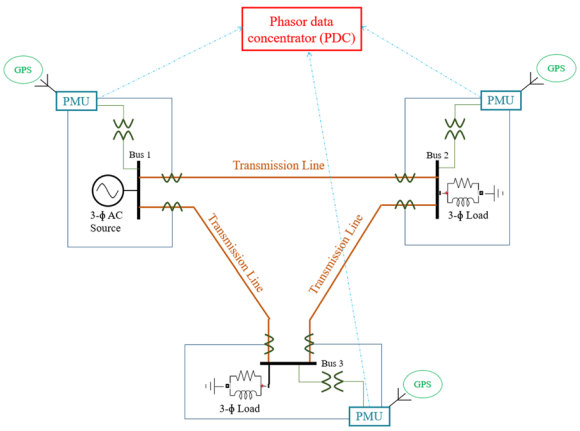

Fig. 5 Single line diagram of three-bus model

simpler, θ_{cpij} is considered as the difference between the positive sequence current phasor angles measured at both ends in line ij, and the maximum value of θ_{cpij} among all the positive sequence current phasor angles is considered as the faulty branch. In this case, the values of θ_{cp23} and θ_{cp31} are found to be 3.98 rad and 0.56 rad. The maximum value of θ_{cpij} is 3.98 rad, which indicates that faulty branch is line 2–3.

Extensive simulation studies were performed with various types of faults at different fault distances, fault inception angles and fault resistance. The fault bus detection and faulty branch detection algorithm proved to be successful in detecting faults within 1 cycle of the nominal frequency for the three-bus system.

4 Fault classification strategy using PMUs

Fault classification is the next step that follows in the fault analysis procedure. In the proposed work, the difference in sending and receiving end current phasors at the two buses of the faulty branch is calculated and is termed as the differential current phasor (I_f). Then the zero, positive and negative sequence components of the differential current phasor magnitudes are noted as α_0, α_1 and α_2 respectively. The zero, positive and negative sequence phasor angles of the differential current are noted as β_0, β_1 and β_2 respectively. The following quantities are calculated for the fault classification algorithm: $\gamma_{i01} = \alpha_0/\alpha_1$, $\gamma_{i21} = \alpha_2/\alpha_1$, $\delta_{i01} = (\beta_0 - \beta_1)$, and $\delta_{i21} = (\beta_2 - \beta_1)$.

The ratios of the phasor magnitudes and the algebraic difference in the phasor angles are indicative of the type of fault and are hence used for fault classification. First, γ_{i01} is computed. If this value is equal to unity, it indicates a line-ground fault, where the magnitudes of zero, positive and negative sequence components of the differential current are all equal. The type of fault is further classified using the value of δ_{i01}. If the value of γ_{i01} is a value greater than zero and less than unity, it indicates that the positive sequence component of the

Table 1 Verification of Fault Analysis algorithm for BG fault in Three-Bus System

Fault Detection

Fault Created	V_1^- (kV)	V_2^- (kV)	V_3^- (kV)	I_{Max}^+ (kA)	Are all of (V_1^-, V_2^-, V_3^-) > 0? (or) $I_{Max}^+ > \tau_B$ (Y – Fault or Unbalance Loading N – No Fault)	I_{12}^- (kA)	I_{23}^- (kA)	I_{31}^- (kA)	$I_{Max}^- = \max(I_{12}^-, I_{23}^-, I_{31}^-)$	$I_{Max}^+ > \tau_B$ (or) $I_{Max}^- > \tau_i$ (Y – Fault, N–Unbalanced Loading)	V_1^+ (kV)	V_2^+ (kV)	V_3^+ (kV)	Min V^+ (kV)	Faulty Bus Detected	θ_{cp12} (rad)	θ_{cp23} (rad)	θ_{cp31} (rad)	Max θ_{cp} (rad)	Faulted Line Detected
BG, Line 2–3, 90 km from Bus 2, FR = 10 Ω, FIA = 72^0	11.58	56.13	54.31	–	Y	0.03	1.33	0.03	1.33	Y	375.63	371.25	370.06	370.06	Bus 3	0.00	3.98	0.56	3.98	Line 23

Fault Classification

Fault Created	α_{i0} (A)	α_{i1} (A)	α_{i2} (A)	β_{i0} (deg)	β_{i1} (deg)	β_{i2} (deg)	γ_{i01} (α_{i0}/α_{i1})	δ_{i01} (β_{i0}- β_{i1}) (deg)	Is $\gamma_{i01} \approx 1$?	Fault type	Is $\delta_{i01} \approx -120^0$?	Fault classified
BG, Line 2–3, 90 km from Bus 2, FR = 10 Ω, FIA = 72^0	1200.593	1070.128	1178.631	−69.259	61.735	174.085	1.121	−130.994	Y	LG	Y	BG

Fault Location

Fault Created	V_a^+ (kV)	V_b^+ (kV)	I_{ab}^+ (A)	I_{ba}^+ (A)	Calculated distance ($d_{calculated}$)	Error (%)
BG, Line 2–3, 90 km from Bus 2, FR = 10 Ω, FIA = 72^0	366.209–60.950i	368.203–45.920i	2.441–495.572i	−470.969 + 421.825i	87.685	−1.16

differential current phasor is distributed between the zero and negative sequence components. This is therefore indicative of a double line-ground fault and the type of fault is further classified using the value of δ_{i21}. If the ratio of γ_{i21} is equal to unity, it indicates that zero sequence components are absent in the differential current phasor. This condition indicates a double-line fault and the type of fault is further classified using the value of δ_{i21}. If none of the conditions are satisfied, it is a symmetric fault. Fig. 6 depicts the fault classification algorithm in detail.

4.1 Line-ground (LG) fault

Once the fault has been indicated as an LG Fault, the corresponding phasor angle difference (δ_{i01}) is computed. For an AG fault, the values of I_{fb} and I_{fc} would be zero. Hence, the zero, positive and negative sequence components of the differential current phasor would all be equal. Hence, the value of δ_{i01} is 0^0. In the case of BG and CG faults, the phasors are rotated by angles of -120^0 (or 240^0) and 120^0 respectively. Hence, the value of δ_{i01} is 240^0 in the case of BG fault, and 120^0 in the case of CG fault.

4.2 Line-line (LL) fault

Once the fault has been indicated as an LL Fault, the phasor angle difference (δ_{i21}) is computed. For example, in the case of an AB fault, $I_{fb} = -I_{fa}$, and $I_{fc} = 0$. By calculating the individual symmetrical components, the positive and negative sequence current phasors are obtained as $I_{fa}(1\text{-}a)$ and $I_{fa}(1\text{-}a^2)$ respectively. The value of positive sequence current phasor angle would be $(\phi\text{-}30^0)$, where ϕ is the phasor angle of I_{fa}. Similarly, the value of negative sequence current phasor angle would be $(\phi + 30^0)$. For AB fault, the phasor angle difference (δ_{i21}) would be 60^0. Similarly, for a BC fault, the value of δ_{i21} would effectively be $(60^0 + 120^0)$, which is equal to 180^0, and for a CA fault, the value of δ_{i21} would be -60^0.

4.3 Double line-ground (LLG) fault

Once the fault has been indicated as an LLG Fault, the phasor angle difference (δ_{i21}) is computed. For example, in the case of an ABG fault, I_{fa} and I_{fb} are non-zero, while $I_{fc} = 0$. The positive and negative sequence current phasors are obtained as $(I_{fa}\text{-}aI_{fb})$ and $(I_{fa}\text{-}a^2I_{fb})$ respectively. As in the case of LL faults, the value of δ_{i21} would be 60^0. Similarly, for a BCG fault, the value of δ_{i21} would be 180^0 and for a CAG fault, the value of δ_{i21} would be -60^0.

For validating the proposed algorithm, a case study of an AB fault (occurring at 120 km from Bus 2) on line 2–3 of the three-bus system is taken (discussed in Table 2). The value of FIA considered is 108^0 and fault impedance is 10 Ω. The calculated magnitude values of the zero, positive and negative sequence components of the differential current phasor are $\alpha_0 = 0.078$ A, $\alpha_1 = 3424.536$ A and $\alpha_2 = 3722.221$ A respectively. Similarly, the computed current phasor angle values for each symmetrical component are calculated as $\beta_0 = 56.282°$, $\beta_1 = 43.566°$ and $\beta_2 = 102.827°$. The ratio γ_{i01} is computed and found to be equal to 0. Next, γ_{i21} is computed as 1.087. This condition denotes an LL fault. The value of δ_{i21} is computed to be 59.261°. From the value of δ_{i21}, it is concluded that the fault is an AB fault.

Extensive simulation studies have been performed, and few of the test scenarios have been presented in Table 1 and Table 2. The proposed algorithm for fault

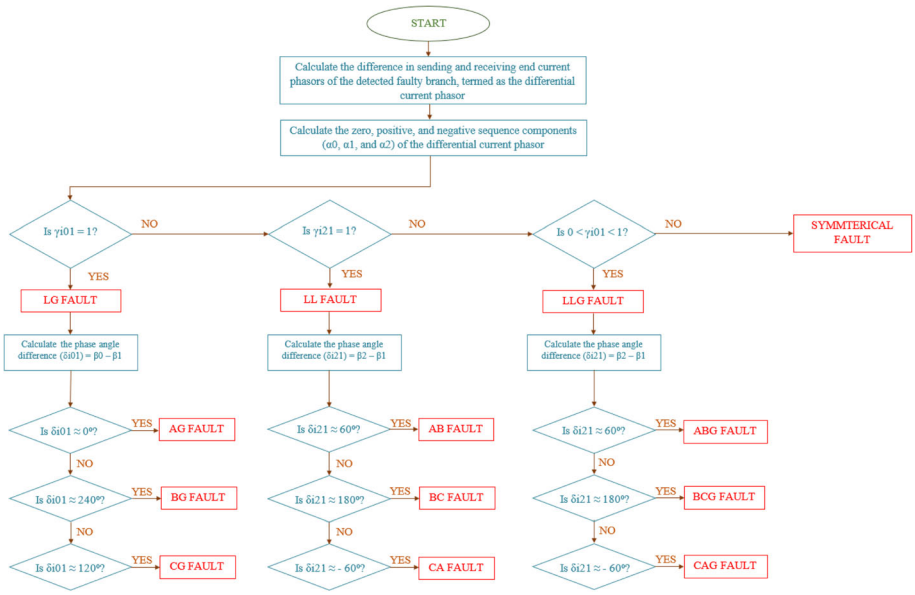

Fig. 6 Fault Classification Algorithm

Table 2 Verification of Fault Analysis algorithm for AB fault in Three-Bus System

Fault Detection

Fault Created	V_1^- (kV)	V_2^- (kV)	V_3^- (kV)	Are all of (V_1^-, V_2^-, V_3^-) > 0 (or) $I_{Max}^+ > \tau_B$ (Y – Fault or Unbalance Loading N – No Fault)	I_{12}^- (kA)	I_{23}^- (kA)	I_{31}^- (kA)	$I_{Max}^- = \max(I_{12}^-, I_{23}^-, I_{31}^-)$	$I_{Max}^+ > \tau_B$ (or) $I_{Max}^- > \tau_i$ (Y – Fault, N–Unbalanced Loading)	V_1^+ (kV)	V_2^+ (kV)	V_3^+ (kV)	Min V^+ (kV)	Faulty Bus Detected	θ_{cp12} (rad)	θ_{cp23} (rad)	θ_{cp31} (rad)	Max θ_{cp} (rad)	Faulted Line Detected
AB, Line 2–3, 120 km from Bus 2, FR = 10 Ω, FIA = 108^0	33.29	62.72	64.33	Y	0.07	3.79	0.08	3.79	Y	353.75	280.56	265.00	265.00	Bus 3	0.00	3.35	0.07	3.35	Line 23

Fault Classification

Fault Created	α_{i0} (A)	α_{i1} (A)	α_{i2} (A)	β_{i0} (deg)	β_{i1} (deg)	β_{i2} (deg)	γ_{i01} (α_{i0}/α_{i1})	γ_{i21} (α_{i2}/α_{i1})	δ_{i21} (β_{i2}- β_{i1}) (deg)	Is $\gamma_{i01} \approx 1$?	Is $\gamma_{i21} \approx 1$?	Fault type	Is $\delta_{i01} \approx 60$?	Fault classified
AB, Line 2–3, 120 km from Bus 2, FR = 10 Ω, FIA = 108^0	0.078	3424.536	3722.221	56.282	43.566	102.827	0.00	1.087	59.261	N	Y	LL	Y	AB

Fault Location

Fault Created	V_a^+ (kV)	V_b^+ (kV)	I_{ab}^+ (A)	I_{ba}^+ (A)	Calculated distance ($d_{calculated}$)	Error (%)
AB, Line 2–3, 120 km from Bus 2, FR = 10 Ω, FIA = 108^0	275.231–54.399i	261.035–45.679i	153.492–1585.769i	− 562.477 + 1803.866i	120.961	0.48

classification proved to be robust and accurate in the distinction of all types of faults, with a processing time of 1–2 cycles (after fault inception) of the nominal frequency.

5 Fault location strategy using PMUs

For obtaining the complete fault information on the transmission line, a fault location technique has been presented which does not require any additional information beyond the synchrophasor measurements that are utilized for fault detection and classification. Fault location techniques proposed in earlier works [16–18] employ sophisticated algorithms to locate a fault. The most commonly used fault location techniques are impedance-based fault location methods. Single-ended impedance-based fault location algorithm techniques have several disadvantages [29]. They only work when the fault voltages and currents recorded by the PMU correspond to the faulted line. They also provide inaccurate results in the presence of tapped lines or three terminal lines. This situation necessitates the need for double ended fault location algorithms which are highly accurate but need measurements from both ends of the line. This can only be achieved when PMUs are present in all the buses. Hence, the proposed scheme takes advantage of data available from each bus of the system to enable accurate fault location. The voltage and current phasors at the two buses in the faulted branch (termed hereafter as Bus a and Bus b) are taken. From these phasor quantities, the positive sequence components of the voltage and current phasors are extracted. Here, the positive sequence components are used because they are non-zero for all types of faults (zero sequence components do not exist for non-ground faults and negative sequence components do not exist for symmetrical faults).

Fig. 7 shows the positive sequence circuit of the faulty transmission line. Here V_a^+ and V_b^+ represent the positive sequence components of voltage phasors at buses a and b. Similarly, I_{ab}^+ and I_{ba}^+ represent the positive sequence component of line current phasors flowing from buses a and b. Z_{pab} represents the positive sequence impedance of the faulty branch (identified previously in the faulty branch detection algorithm).

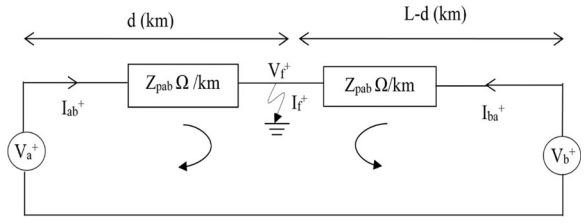

Fig. 7 Positive sequence circuit of transmission line

From the case studies presented in Tables 1-3, eq. (2) is independent of FIA, fault distance and fault resistance and hence this algorithm can be used for all types of fault resistance and fault types.

In the circuit shown in Fig. 7, a fault occurs at a distance d km from the bus a on a line of length L km. To find the distance d without involving the unknown fault voltage (V_F^+), Kirchoff's Voltage Law (KVL) is applied for the two loops (shown in Fig. 7).

Therefore,

$$V_a^+ - I_{ab}^+ Z_{pab} d = V_F^+$$

$$V_b^+ - I_{ba}^+ Z_{pab} (L - d) = V_F^+$$

Eliminating V_F from the above two equations,

$$d = \frac{V_a^+ - V_b^+ - I_{ba}^+ Z_{pab} L}{Z_{pab}\left(I_{ba}^+ + I_{ab}^+\right)} \quad (2)$$

For explaining the fault location procedure, a case study is assumed where a BG fault occurs at 90 km (from Bus 2) in line 2–3 of the three-bus system (discussed in Table 1). The value of FIA considered is 72^0 and fault impedance is 10 Ω. The positive sequence voltage phasors at Bus 2 and Bus 3 (termed as V_a^+ and V_b^+ respectively) and the current phasors flowing from both ends of the line (termed as I_{ab}^+ and I_{ba}^+ respectively) are used to calculate the fault distance. The required values are obtained as V_a^+ = (366.209 - 60.950i) kV, V_b^+ = (368.203 - 45.920i) kV, I_{ab}^+ = (2.441–495.572i) A, I_{ba}^+ = (– 470.969 + 421.825i) A. Applying the relation shown in eq. (2), the fault location is calculated as 87.685 km from Bus 2, and the fault is created at 90 km from Bus 2. This calculation gives an error of only – 1.16% in fault distance estimation.

6 Results and discussion

The proposed methodologies for fault detection, classification and location have been validated successfully by implementing the algorithm on a larger power system, the WSCC nine bus model. Extensive simulation studies have been performed with varying fault conditions and fault parameters such as fault impedance and fault distance. Transmission line faults are simulated in MATLAB-SIMULINK to obtain various fault conditions. The results of a few scenarios from the studies conducted on the WSCC nine bus system are presented below to demonstrate the efficacy of the algorithms.

The WSCC nine bus model (shown in Fig. 8) is a standard nine bus model used in power system studies. The rating of each generator is 400 kV, 50 Hz. The power ratings of each generator are as follows: Bus 1 has a power rating of 163 MW, 6.7 Mvar; Bus 2 has a power rating of 71.6 MW, 27 Mvar; and Bus 3 has a power rating of 85 MW, 10.9 Mvar.

Table 3 Verification of Fault Analysis algorithm for ABG fault in WSCC Nine Bus System

Fault Detection, Bus identification and Faulted Line Identification

Fault Created	V_1^- (kV)	Are all of (V_1^-, V_2^-, V_3^-, V_4^-, V_5^-, V_6^-,V_7^-,V_8^-,V_9^-) > 0 (or) $I_{Max}^+ > \tau_B$?	I_{14}^- (kA)	I_{27}^- (kA)	I_{93}^- (kA)	I_{46}^- (kA)	I_{54}^- (kA)	I_{69}^- (kA)	I_{78}^- (kA)	I_{75}^- (kA)	I_{98}^- (kA)	$I_{Max}^- = \max(I_{14}^-, I_{27}^-, I_{93}^-, I_{46}^-, I_{54}^-, I_{69}^-, I_{78}^-, I_{75}^-, I_{98}^-)$	$I_{Max}^+ > \tau_B$ (or) $I_{Max}^- > \tau_i$ (Y – Fault, N – Unbalanced Loading)
ABG, Line 4–1, 80 km from Bus 1, FR = 1 Ω, FIA = 36^0	22.31	Y	5.64	0.01	0.01	0.05	0.05	0.03	0.02	0.03	0.02	5.64	Y

Fault Created	V_1^+ (kV)	V_2^+ (kV)	V_3^+ (kV)	V_4^+ (kV)	V_5^+ (kV)	V_6^+ (kV)	V_7^+ (kV)	V_8^+ (kV)	V_9^+ (kV)	Min V^+ (kV)	Faulty Bus Detected
ABG, Line 4–1, 80 km from Bus 1, FR = 1 Ω, FIA = 36^0	291.87	316.90	318.15	163.29	192.40	195.11	229.52	228.04	236.45	163.29	Bus 4

Fault Created	θ_{cp14} (rad)	θ_{cp27} (rad)	θ_{cp93} (rad)	θ_{cp46} (rad)	θ_{cp54} (rad)	θ_{cp69} (rad)	θ_{cp78} (rad)	θ_{cp75} (rad)	θ_{cp98} (rad)	Max θ_{cp} (rad)	Faulted Line Detected
ABG, Line 4–1, 80 km from Bus 1, FR = 1 Ω, FIA = 36^0	1.57	0.00	0.00	0.12	0.13	0.00	0.00	0.00	0.00	1.57	Line 41

Fault Classification

Fault Created	α_{i0} (kA)	α_{i1} (kA)	α_{i2} (kA)	β_{i0} (rad)	β_{i1} (rad)	β_{i2} (rad)	γ_{i21} (α_{i2}/α_{i1})	γ_{i01} (α_{i0}/α_{i1})	δ_{i21} (β_{i2}-β_{i1}) (deg)	Is $\gamma_{i01} \approx 1$?	Is $\gamma_{i21} \approx 1$?	Is $0 < \gamma_{i01} < 1$?	Fault type	Is $\delta_{i21} \approx 60^0$?	Fault classified
ABG, Line 4–1,80 km from Bus 1	1.80	7.15	5.64	0.71	1.59	2.59	0.78	0.25	56.14	N	N	Y	LLG	Y	ABG

Fault Location

Fault Created	V_a^+ (kV)	V_b^+ (kV)	I_{ab}^+ (kA)	I_{ba}^+ (kA)	Distance (km)	Error (%)
ABG, Line 4–1, 80 km from Bus 1	291.815–5.752i	135.99–90.373i	1.686–6.781i	1.518 + 0.370i	79.76	−0.12

There are nine EHV transmission lines in the power network, and each is modeled as a distributed parameter block with the following positive and negative sequence parameters: $R = 0.0234\ \Omega$/km, L = 95.1 mH/km, C = 1.24uF/km. The zero sequence components of the line are: $R_0 = 0.3885\ \Omega$/km, $L_0 = 3.25$ mH/km, $C_0 = 8.45$ nF/km respectively. The threshold values were determined experimentally. The value of the threshold (τ_B) is 2.17 kA, whereas the value of the threshold (τ_i) is 0.43 kA. Furthermore, for a 1000 MVA, 400 kV system base, 0.3 p.u of current corresponds to 0.43 kA, and 1.5 p.u of current corresponds to 2.17 kA.

6.1 Fault scenario in the WSCC nine bus system model

A case of an ABG fault at 80 km (from Bus 1) in line 1–4 in the WSCC system (Table 3) is considered for demonstration. The value of FIA considered is 36^0 and fault impedance is 1 Ω. The individual negative sequence components of bus voltage phasors are non-zero. It is thus ascertained that there is a presence of a fault or unbalanced loading. The maximum value of the negative sequence component (5.64 kA) is greater than the threshold value (τ_i), which indicates the presence of a fault. From the tabulated values of positive sequence voltage phasor magnitudes at buses 1 to 9, it is determined that the faulted bus in the system is Bus 4, as it has the least magnitude value. The values of positive sequence current phasor angle differences of line currents (i.e., the lines connected to Bus 4) are obtained as $\theta_{cp46} = 0.12$ rad, $\theta_{cp45} = 0.13$ rad and $\theta_{cp14} = 1.57$ rad for line 4–6, line 4–5 and line 1–4 respectively. This phasor angle difference indicates that the faulted line is line 1–4.

For fault classification, the calculated magnitude values of the zero, positive and negative sequence components of this current phasor are $\alpha_0 = 1.8$ kA, $\alpha_1 = 7.15$ kA, and $\alpha_2 = 5.64$ kA respectively. Similarly, the computed phasor

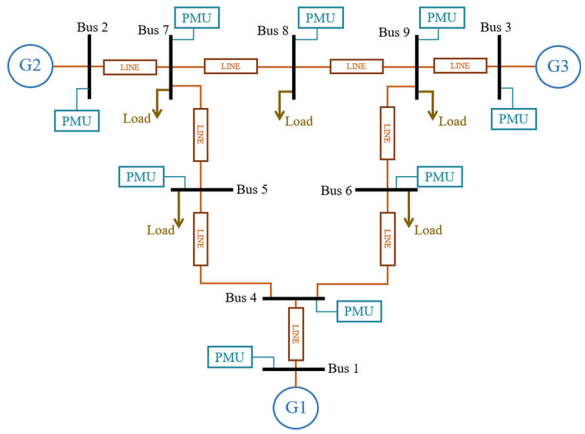

Fig. 8 Single Line Diagram of WSCC Nine Bus system

angle values for each symmetrical component are calculated as $\beta_0 = 0.71$ rad, $\beta_1 = 1.59$ rad, and $\beta_2 = 2.59$ rad. The ratio γ_{i01} is computed as 0.25. Next, the ratio γ_{i21} is calculated as 0.78. It is observed that neither γ_{i01} nor γ_{i21} is equal to unity, but $0 < \gamma_{i01} < 1$. Hence, it is indicative of an LLG fault and the value of δ_{i21} is computed as 56.14°. Furthermore, the value of δ_{i21} is checked and $\delta_{i21} \approx 60°$. Hence, it is concluded that the fault is an ABG fault.

For fault location, the buses 1 and 4 are considered. The required values are obtained as $V_a^+ = (291.815–5.752i)$ kV and $V_b^+ = (135.99–90.373i)$ kV respectively. Similarly, the value of I_{ab}^+ is (1.686–6.781i) kA and value of I_{ba}^+ is (1.518 + 0.37i) kA. By substituting these values in eq. (2), the fault location is calculated as 79.76 km from Bus 1, where the actual fault is created at 80 km from Bus 1. This calculation gives an error of − 0.12% in fault distance estimation.

Similar to the three-bus system, comprehensive fault detection, classification and location studies of different types of faults in the WSCC nine bus system were performed, and the algorithms proved to be robust and successful. It was possible to distinguish between transients, non-fault conditions and persistent fault conditions which are discussed in the future subsections. For the WSCC nine bus system, the fault detection was accomplished successfully within one-half cycle of nominal frequency (after fault inception), and fault classification and location were also completed within 2 cycles of the nominal frequency.

6.2 Transient events

Some of the common transient events that occur in a power system are voltage drop because of overloading and generator outage. The condition checks involving negative sequence components and their threshold values help to distinguish between the faulted condition and transient events. Only the negative sequence components exist when there is an unbalance amongst the three phases of the system. When there is a generator outage, though the overall voltage of the system might drop, the effect is uniform in all the three phases. Hence, during this transient event, negative sequence component of bus voltages will not exist. So, generator outage will not be identified as a fault in the transmission system. Similarly, voltage drops caused by overloading is uniform in all the three phases. Even if it is not uniform in all the three phases, the unbalance in the system is much less compared to a fault event. Hence, the negative sequence voltage component will be very less or none in this case. During an unbalanced fault event, the fault current in the faulted phase of the line is enormous (ranging from 2 p.u to more than 40 p.u) which is caused by corresponding unbalance in the voltage level as well. Hence, the negative sequence components arising from a faulted event is large and very significant compared to unbalanced loaded conditions. Hence, the threshold setting (which would be obtained based on experimental studies of the system) based on the negative sequence components helps distinguish transient events from faulted events.

6.3 Normal loading condition

When there is no fault in the system, the voltage and currents are expected to be nearly balanced. Hence, the negative sequence component of the voltage phasors will be nearly zero and the positive sequence current magnitudes would be around the loadable limit of the line. Consider a normal loading condition or no-fault system condition in the WSCC nine bus system (discussed in Table 4). The value of negative sequence components of

Table 4 Verification of Fault Detection algorithm in WSCC Nine Bus System

Fault Detection															
Fault Created	V_1^- (kV)	I_{Max}^+ (kA)	Are all of (V_1^-, V_2^-, V_3^-,V_4^-,V_5^-, V_6^-,V_7^-,V_8^-,V_9^-) > 0 (or) $I_{Max}^+ > \tau_B$	I_{14}^- (kA)	I_{27}^- (kA)	I_{93}^- (kA)	I_{46}^- (kA)	I_{54}^- (kA)	I_{69}^- (kA)	I_{78}^- (kA)	I_{75}^- (kA)	I_{98}^- (kA)	$I_{Max}^- = \max(I_{14}^-$, I_{27}^-, I_{93}^-, I_{46}^-, I_{54}^-, I_{69}^-, I_{78}^-, I_{75}^-, I_{98}^-)	$I_{Max}^+ > \tau_B$ (or) $I_{Max}^- > \tau_i$ (Y – Fault, N – Unbalanced Loading)
Unbalanced Load at Bus 1	2.05	0.83	Y	0.01	0.01	0.01	0.01	0.01	0.01	0.01	0.01	0.01	0.01		N
No Fault	0.00	0.873	N	–	–	–	–	–	–	–	–	–	–		–

bus voltage phasors (V_1^-, V_2^-, V_3^-, V_4^-, V_5^-, V_6^-, V_7^-, V_8^- and V_9^-) are all equal to zero. Also, the maximum value of positive sequence current phasors in all the lines is computed. The value of $I_{Max}^+ = 0.873$ kA, which is less than the threshold value (τ_B). Hence, the algorithm indicates that there is no fault in the system.

6.4 Unbalanced loading condition

During an unbalanced loading condition, there is the presence of negative sequence voltage and line currents, but unlike a fault condition, they are small in magnitude. A case of unbalanced loading is taken at Bus 1 in the WSCC nine bus system (discussed in Table 4), where the magnitudes of negative sequence components of all the bus voltage phasors (V_1^-, V_2^-, V_3^-, V_4^-, V_5^-, V_6^-, V_7^-, V_8^- and V_9^-) are all greater than zero. Due to a limitation in space, these values are not presented in Table 4. This condition indicates the presence of unbalanced loading or a fault condition. Next, the magnitudes of negative sequence components of the line current phasors are also obtained as: $I_{14}^- = 0.01$ kA, $I_{27}^- = 0.01$ kA and $I_{93}^- = 0.01$ kA, $I_{46}^- = 0.01$ kA, $I_{54}^- = 0.01$ kA, $I_{69}^- = 0.01$ kA, $I_{78}^- = 0.01$ kA, $I_{75}^- = 0.01$ kA and $I_{98}^- = 0.01$ kA. It is observed that the maximum magnitude of the negative sequence component (0.01 kA) is less than the threshold value (τ_i). This condition is therefore detected as an unbalanced loading (not a fault condition).

6.5 Other advantages

The major advantage of the proposed algorithm is that it can detect and classify faults with high accuracy and speed as demonstrated in this paper. Apart from being able to distinguish between the transient event and persistent fault, another advantage of the proposed technique is that the system remains protected even when one of the PMU fails. This is because the fault detection and faulted line identification is based on the presence of negative sequence voltage in the system and lowest positive sequence bus voltage. When PMU present at one end of the faulted line fails, the PMU at the other end of fault line will still record the presence of negative sequence voltages and will have lower bus voltage than the other buses in the system. Hence, the loss or damage of a PMU does not jeopardize the power system, which is an important feature. The proposed fault location algorithm utilizes PMU measurements from both ends of the faulted line and is shown to be more accurate than other impedance-based techniques. These features are additional advantages for PMU placement at all the buses in the network.

6.6 Time of operation and feasibility

Our proposed work completes the three stages of fault analysis within 3–5 cycles of nominal frequency, which is quite fast compared to other works in the literature that implement optimal PMU placement algorithms. For instance, in [27], the authors have undertaken a probabilistic study with optimal PMU placement, wherein the most credible contingencies are evaluated for fault analysis; consequently, the total time for the execution of fault analysis procedure is reported to be 0.4 s, which is largely due to the processing time required to detect the fault due to the limited number of PMUs. The ability to perform rapid and accurate fault detection, classification and location strengthen the practical applicability of the proposed methodology.

The system monitored by a single PDC is mainly limited by the communication infrastructure and by the computational capability of the processors. Hence, it is not feasible to have vast geographical regions monitored by a single PDC. Equivalent Thevenin impedances can be used at the periphery of the system to represent the rest of the grid.

7 Conclusion

With the increasing complexity of modern power systems, the incorporation of WAPS is necessary for power system protection. PMUs are highly preferred for this application because of the numerous benefits they provide. A novel methodology for rapid and high accuracy fault detection, classification, and location using PMUs is proposed in this paper. The presence of PMUs at all the buses provides several advantages and increases the accuracy of the fault analysis process. The algorithm can distinguish between fault event and other transient events such as overloading, unbalanced loading and generator outages. The robustness of the fault detection algorithm and the ability of the proposed methodology for fault analysis to be extended to other systems are some of its key advantages. The proposed algorithms are validated by extensive simulation studies involving a variety of faults at different distances, fault impedances and fault inception angles on two test systems, a three-bus power system and the WSCC nine-bus power system. From the studies performed, the results indicate that a fault occurring anywhere in the system can be correctly detected, classified and located. The fault detection algorithm can detect the presence of a fault within one power cycle. The speed of operation of the proposed algorithm facilitates faster restoration of faulty branches, hence reducing the power outage time and enhancing the reliability of the power system.

Authors' contributions

PR and NAS have developed and modeled the proposed algorithm. MB has made substantial contributions to simulate WSCC nine-bus network. MJBR has been the technical adviser for the total work and DKM has supported us

in interpreting the simulation results for fault analysis. All authors read and approved the final manuscript.

Competing interests
The authors declare that they have no competing interests.

Author details
[1]Department of Electrical and Computer Engineering, University of Illinois at Urbana Champaign, Champaign, IL, USA. [2]Department of Electrical and Computer Engineering, University of Texas at Austin, Austin, TX, USA. [3]Department of Electrical and Electronics Engineering, National Institute of Technology, Tiruchirappalli, Tamilnadu 620015, India. [4]Department of Electrical and Electronics Engineering, Birla Institute of Technology, Mesra, Ranchi 835215, India.

Received: 24 August 2017 Accepted: 15 March 2018
Published online: 16 April 2018

References
1. Ram, B., & Vishwakarma, D. N. (2005). *Power system protection and switchgear* (pp. pp6–9–119–123). New Delhi: Tata McGraw-Hill publication company limited.
2. Spoor, D., & Zhu, J. G. (2006). Improved single-ended traveling-wave fault location algorithm based on experience with conventional substation transducers. *IEEE Transactions on Power Delivery, 21*(3), 1714–1720.
3. Samantaray, S. R., Dash, P. K., & Panda, G. (2007). Distance relaying for transmission line using support vector machine and radial basis function neural network. *Electrical power and energy systems, 29*(7), 551–556.
4. Vazquez-Martinez, E. (2003). A travelling wave distance protection using principle component analysis. *International Journal of Electric Power and Energy Systems, 25*(6), 471–479.
5. Youssef, A. S. (2004). Combined fuzzy-logic wavelet-based fault classification technique for power system relaying. *IEEE Transactions on Power Delivery, 19*(2), 582–589.
6. Dong, X., Kong, W., & Cui, T. (2009). Fault classification and faulted-phase selection based on the initial current travelling wave. *IEEE Transactions on Power Delivery, 24*(2), 552–559.
7. Torabi, N., Karrari, M. Menhaj, M.B. & Karrari, S. (2012). Wavelet Based Fault Classification for Partially Observable Power Systems. Power and Energy Engineering Conference (APPEEC), Asia-Pacific region, 1–6.
8. Ferrero, S. (1995). Sangiovanni & Zapitelli, E. *A fuzzy set approach to fault type identification in digital relaying IEEE Transactions on Power Delivery, 10*(1), 169–175.
9. Seethalekshmi, K., Singh, S. N., & Srivastava, S. C. (2012). A classification approach using support vector machines to prevent distance relay Maloperation under power swing and voltage instability. *IEEE Transactions on Power Delivery, 27*(3), 1124–1133.
10. Song, Y. H., Xuan, Q. X., & Johns, A. T. (1997). Comparison studies of five neural network based fault classifiers for complex transmission lines. *Electrical Power Systems Research, 43*(2), 125–132.
11. Poeltl, M., & Frohlich, K. (1999). Two new methods for very fast fault type detection by means of parameter fitting and artificial neural networks. *IEEE Transactions on Power Delivery, 14*(4), 1269–1275.
12. Pradhan, A. K., Dash, P. K., & Panda, G. (2001). A fast and accurate distance relaying scheme using an efficient radial basis function neural network. *Electrical Power System Research, 60*(1), 1–8.
13. Mahanty, R. N., & Dutta Gupta, P. B. (2004). Application of RBF neural network to fault classification and location in transmission lines. *IEEE Proceedings on Generation, Transmission and Distribution, 151*(2), 201–212.
14. Ramesh, L., Chowdhury, S.P. & Chowdhury, S. (2010). Wide area monitoring protection and control - A comprehensive application review. 10th IET International Conference on Developments in Power System Protection, Manchester.
15. Phadke, G., Ibrahim, M., & Hlibka, T. (1977). Fundamental basis for distance relaying with symmetrical components. *IEEE Transactions on Power Apparatus and Systems, 96*(2), 635–646.
16. Joe-Air, J., Jun-Zhe, Y., Ying-Hong, L., Chih-Wen, L., & Jih-Chen, M. (2000). An adaptive PMU based fault detection/location technique for transmission lines. I. Theory and algorithms. *IEEE Transactions on Power Delivery, 15*(2), 486–493.
17. Joe-Air, J., Lin, Y.-H., Yang, J.-Z., Too, T.-M., & Liu, C.-W. (2000). An adaptive PMU based fault detection/location technique for transmission lines—Part II: PMU implementation and performance evaluation. *IEEE Transactions on Power Delivery, 15*(4), 1136–1146.
18. Liu, C.-W., Lin, T.-C., Yu, C.-S., & Yang, J.-Z. (2012). A fault location technique for two-terminal multisection compound transmission lines using synchronized phasor measurements. *IEEE Transactions on Smart Grid, 3*(1), 113–121.
19. Lin, T.-C., Lin, P.-Y., & Liu, C.-W. (2014). An algorithm for locating faults in three-terminal multisection nonhomogeneous transmission lines using Synchrophasor measurements. *IEEE Transactions on Smart Grid, 5*(1), 38–50.
20. He, Z.Y., Li, X.P., He, W., Liu, Y.P. Zhang, S., Mai, R.K. & Qian, Q.Q. (2013). Dynamic fault locator for three-terminal transmission lines for phasor measurement units. IET Generation, Transmission & Distribution, 7(2), 183–191.
21. Al-Mohammed, A.H., Dammam & Abido, M.A. (2014). Fully Adaptive PMU-Based Fault Location Algorithm for Series-Compensated Lines IEEE Transactions on Power Systems, 29 (5), 2129–2137.
22. Kang, N., & Liao, Y. (2013). Double-circuit transmission-line fault location utilizing synchronized current phasors. *IEEE Transactions on Power Delivery, 28*(2), 1040–1047.
23. Neyestanaki, M. K., & Ranjbar, A. M. (2015). An adaptive PMU-based wide area backup protection scheme for power transmission lines. *IEEE Transactions on Smart Grid, 6*(3), 1550–1559.
24. He, Z. Y., Mai, R. K., He, W., & Qian, Q. Q. (2011). Phasor-measurement-unit-based transmission line fault location estimator under dynamic conditions. *IET Generation, Transmission & Distribution, 5*(11), 1183–1191.
25. Gopakumar, P., Reddy, M. J. B., & Mohanta, D. K. (2015). Transmission line fault detection and localisation methodology using PMU measurements. *IET Generation, Transmission & Distribution, 9*(11), 1033–1042.
26. Zare, J., Aminifar, F., & Sanaye-Pasand, M. (2015). Synchrophasor-based wide-area backup protection scheme with data requirement analysis. *IEEE Transactions on Power Delivery, 30*(3), 1410–1419.
27. Gomez, O., Rios, M. A., & Anders, G. (2014). Reliability-based phasor measurement unit placement in power systems considering transmission line outages and channel limits. *IET Generation, Transmission & Distribution, 8*(1), 121–130.
28. Gopakumar, P., Reddy, M. J. B., & Mohanta, D. K. (2015). Fault detection and localization methodology for self-healing in smart power grids incorporating phasor measurement units. *Electric Power Components and Systems, 43*(6), 695–710.
29. Das, S., Santoso, S., Gaikwad, A. and Patel, M. (2014) "Impedance-based fault location in transmission networks: theory and application," in IEEE Access, *2*, 537–557